A review of simulation and performance modeling tools for the Roman coronagraph instrument

Ewan S. Douglas[a], Jaren N. Ashcraft[a], Ruslan Belikov[b], John Debes[c], Jeremy Kasdin[d,f], John Krist[e], Brianna I Lacy[f], Bijan Nemati[h], Kian Milani[a], Leonid Pogorelyuk[g], A J Eldorado Riggs[e], Dmitry Savransky[i], and Dan Sirbu[b]

[a]University of Arizona, Steward Observatory, Tucson, AZ, USA
[b]NASA Ames Research Center, Moffett Field, CA, USA
[c]Space Telescope Science Institute, Baltimore, MD, USA
[d]University of California San Francisco, San Francisco, CA, USA
[e]Jet Propulsion Laboratory, California Institute of Technology, Pasadena, CA, USA
[f]Princeton University, Department of Astrophysical Sciences, Princeton, NJ, USA
[g]Massachusetts Institute of Technology, Cambridge, MA, USA
[h]University of Alabama in Huntsville, Huntsville, AL, USA
[i]Cornell University, Ithaca, NY, USA

ABSTRACT

The Nancy Grace Roman Space Telescope Coronagraph Instrument (CGI) will be capable of characterizing exoplanets in reflected light and will demonstrate space technologies essential for future missions to take spectra of Earthlike exoplanets. As the mission and instrument move into the final stages of design, simulation tools spanning from depth of search calculators to detailed diffraction models have been created by a variety of teams. We summarize these efforts, with a particular focus on publicly available datasets and software tools. These include speckle and point-spread-function models, signal-to-noise calculators, and science product simulations (e.g. predicted observations of debris disks and exoplanet spectra). This review is intended to serve as a reference to facilitate engagement with the technical and science capabilities of the CGI instrument.

Keywords: Roman, WFIRST, coronagraph, exoplanets, debris disks, modeling, diffraction, instrument yield, simulations

1. INTRODUCTION

The Nancy Grace Roman Space Telescope (Roman)[1] Coronagraph Instrument (CGI) is a technology demonstration[2–5] that will use high-contrast imaging and spectroscopy (coronagraphy), wavefront sensing, and wavefront control,[6,7] to image planets in reflected light.[3] Formerly known as the Wide-Field Infrared Survey Telescope, Roman is orders of magnitude more sensitive than Hubble Space Telescope (HST) or ground-based observatories.[8] Two primary coronagraph technologies will be tested, a Hybrid-Lyot Coronagraph (HLC) coronagraph[9] for high contrast small-field-of-view (FOV) (<0.5 as) imaging, a bow-tie Shaped Pupil Coronagraph (SPC)[10] for spectroscopy and a wide-FOV SPC. The design and preparation for CGI has spawned many new modeling tools to accurately predict performance. This work attempts to summarizes the most common of these tools, both to serve as a roadmap for future potential users of CGI and to aid other missions which may benefit from reuse of the many open source tools which have been shared by CGI science and engineering teams. This review cannot completely capture the simulation work that has gone into developing Roman CGI but it is intended to serve as a starting reference for the community to engage with the technical and science capabilities of the instrument. Additionally, to better understand the context of these tools, we suggest previous works, as well as several papers in these proceedings, that provide detailed descriptions of the design reference mission and typical observing modes.[3,8,11,12]

Further author information: (Send correspondence to E.S.D.)
E.S.D,: E-mail: douglase@arizona.edu

Space Telescopes and Instrumentation 2020: Optical, Infrared, and Millimeter Wave, edited by Makenzie Lystrup, Marshall D. Perrin, Proc. of SPIE Vol. 11443, 1144338 · © 2020 SPIE
CCC code: 0277-786X/20/$21 · doi: 10.1117/12.2561960

Table 1. Partial Listing of Open Source CGI Software Packages and Libraries

Package	Application	References	URL
Observing Scenarios	Complete Observation Simulation	13	https://roman.ipac.caltech.edu/sims/Coronagraph_public_images.html
PROPER	Diffraction Simulation	14, 15	https://github.com/ajeldorado/proper-models/tree/master/wfirst_cgi
FALCO	Coronagraph Simulation	16	https://github.com/ajeldorado/falco-matlab, https://github.com/ajeldorado/falco-python
Lightweight Coronagraph Simulator	Coronagraph Simulation	17	https://github.com/leonidprinceton/LightweightSpaceCoronagraphSimulator
CZT-based Optical Propagation	Diffraction Simulation		https://github.com/ARCExoplanetTechnologies/ACED
WebbPSF	Diffraction Simulation	18, 19	https://github.com/spacetelescope/webbpsf
MSWC	Binary Star Simulation	20, 21	https://github.com/ARCExoplanetTechnologies/MSWC
EXOSIMS	Mission Simulation	22, 23	https://github.com/dsavransky/EXOSIMS
Imaging Mission Database	Mission Planning	24	https://plandb.sioslab.com
Coronagraph convolved Debris Disks	Disk Simulation	25	https://roman.ipac.caltech.edu/sims/Circumstellar_Disk_Sims.html
Known debris disk simulated scenes	Disk Simulation	26	https://roman.ipac.caltech.edu/sims/Chen_WPS.html
direct-imaging-sims + model spectra	Target simulation	27, 28	https://github.com/blacy/direct-imaging-sims, https://www.astro.princeton.edu/~burrows/wfirst/index.html
Giant planet albedo spectra	Target simulation	29	https://wfirst.ipac.caltech.edu/sims/Exoplanet_Characterization.html

2. CORONAGRAPH SIMULATORS

2.1 Observing Scenarios

The most detailed and physically realistic simulations of CGI observations released to date have taken the form of numbered observing scenarios. These are referred to as OSn, e.g., OS9 for the ninth scenario. Physical optics simulations of the instrument including optical surfaces, coronagraphs, and wavefront sensing and control are generated using PROPER.[30,31] The scenarios include speckle time series, derived from wavefront maps produced using Structural-Thermal-Optical-Performance (STOP) modeling of the Roman observatory.[32] The OS model outputs include noisy and noiseless datacubes of coronagraphic intensity images versus time, with injected planets and realistic observing scenarios that include reference stars, and off-axis point spread function (PSF)s for injecting additional targets. These scenario files are available to the public from IPAC.

2.2 FALCO

The FALCO[16] library provides a framework for running wavefront sensing and control algorithms in MATLAB and Python 3. FALCO can use a PROPER[30] model as its truth model in simulations, and examples using the

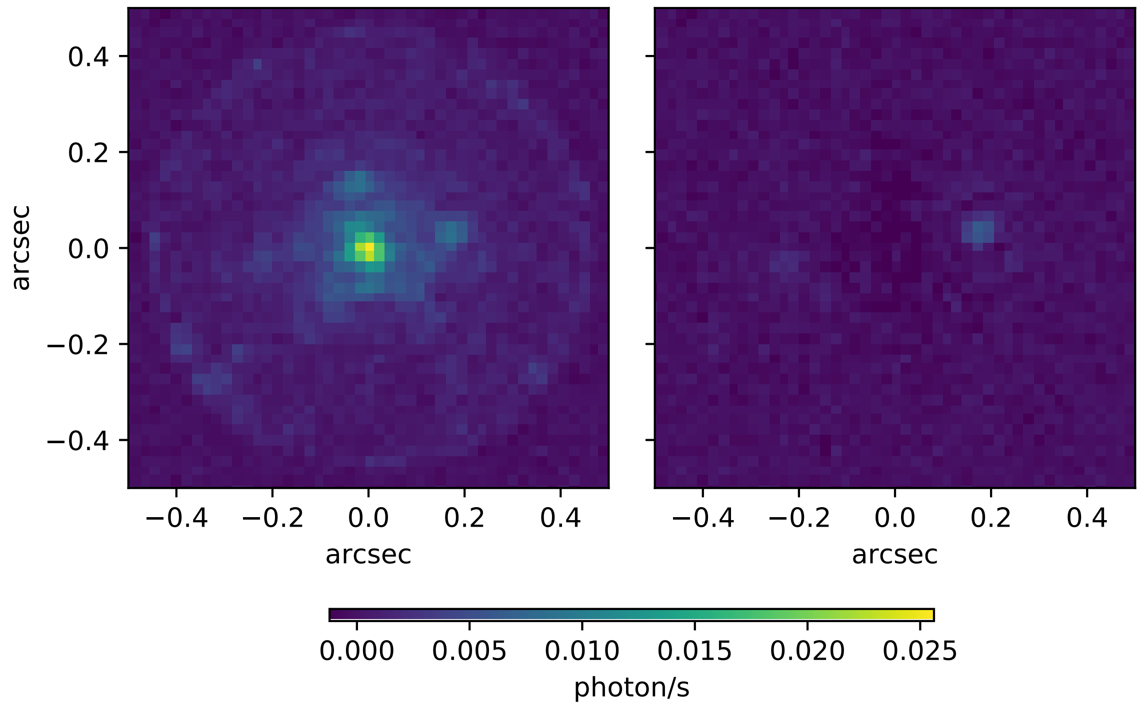

Figure 1. Images of 47 Uma c generated from publicly available OS9 simulations of the HLC including time dependent speckle and detector effects. Left: simulated image with injected planets. Right: the same scene after reference subtraction, showing injected planets at a much higher SNR.

CGI PROPER model are included in the publicly available FALCO repository. Example status window updates for the hybrid Lyot coronagraph are shown in Fig. 2.

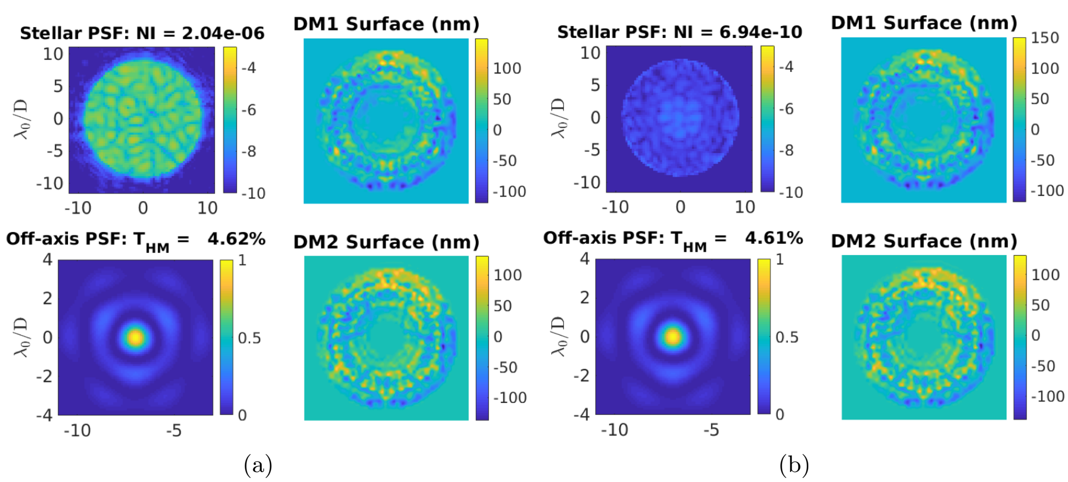

Figure 2. Status report windows from FALCO before (a) and after (b) performing wavefront control using the CGI PROPER model as the truth model. The large starting shapes on the deformable mirrors are the HLC design settings combined with the settings for flattening the starting wavefront errors.

2.3 Lightweight Space Coronagraph Simulator

Based on FALCO,[16] the "Lightweight Space Coronagraph Simulator" computes small linear perturbations about the nominal dark hole instead of propagating the full optical model. It allows quickly simulating observation scenarios with time evolving wavefront error (WFE), Deformable Mirror (DM) drift, low-order wavefront sensing and control (LOWFS/C) residual jitter and high-order wavefront sensing and control (HOWFS/C).[17] The sensitivities to DM commands (the Jacobian) and to WFE were computed in 6 wavelengths using FALCO and remain valid in the linear regime (up to 10 nm phase perturbations). This allows specification of DM voltages, WFE Zernikes, LOWFS residual jitter, detector noise and switching between broadband and narrowband modes. The Python code is designed to run fast and only requires NumPy.[33] Fig. 3 shows an example dark hole time series (left) and dark hole image (right).

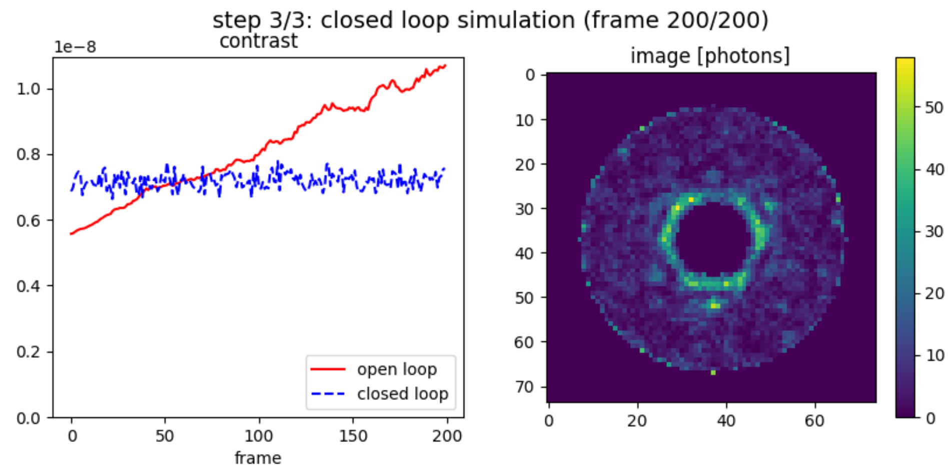

Figure 3. An example of contrast evolution in presence of various wavefront instabilities in a linearized model of Roman-CGI. Left: Closing the loop allows maintaining the contrast throughout the observation. The drift rate is exaggerated to illustrate dark hole maintenance in the worst-case scenario of random walk of Zernike coefficients. Right: A broadband photon-counts image of a single exposure (used to close the contrast loop). See Pogorelyuk et al.[17] for details.

2.4 CZT-based Optical Propagation

The Chirp Z-Transform (CZT) based optical propagation library, developed at Princeton and NASA Ames, implements 2D Fraunhofer and Fresnel diffraction propagation on arbitrarily sampled input and output planes. It provides the same functionality and answer (to within numerical precision) as the more commonly used MFT technique (Matrix Fourier Transform), but is asymptotically faster.

2.5 MSWC

Binary stars represent a special challenge for a diffraction simulation due to the angular separation between the on-axis target and its off-axis companion. The off-axis companion can contribute stellar leakage due to optical aberrations at high-frequencies for every component in the optical train. The Multi-Star Wavefront Control (MSWC) package can be used to simulate binary stars, predict the expected leakage for different binary star imaging scenarios, and determine if the contrast leakage due to the off-axis companion introduces a background contrast floor for a particular Roman CGI imaging mode. This can flag known binaries as benign or requiring suppression. Depending on the Roman CGI imaging mode, wavefront control techniques may remove the binary companion's leakage.[20,21,34]

2.6 WebbPSF

WebbPSF[18,35] is a PSF simulation tool originally developed for *James Webb Space Telescope* (JWST) in Python. Basic SPC modes are currently included in WebbPSF[36*] and are in the process of being updated to match current filters and mask designs.

*https://www.stsci.edu/jwst/science-planning/proposal-planning-toolbox/psf-simulation-tool

3. YIELD

3.1 Yield Calculator

Nemati[37,38] developed an analytic model of instrument sensitivity that calculates the time-to-SNR for known radial velocity (RV) exoplanets. This model has been widely used by the project team as an Excel spreadsheet and is now publicly available as part of EXOSIMS (see below).

3.2 EXOSIMS

EXOSIMS[22] is an open source, full exoplanet imaging mission simulation tool, which generates a survey ensemble of possible exoplanet detections given an underlying universe (e.g. exoplanet phase curves and occurrence rates) and observatory properties such as orbit, optical system performance, and background sources.

3.3 Imaging Mission Database

The online Cornell Space Imaging and Optical Systems Lab *Imaging Mission Database*uses stellar and RV exoplanet physical properties.[39] As shown in Fig. 4, these properties can be combined in joint distributions and compared to the instrumental sensitivity floor (blue curve) to assess the frequency of detection in an observation. Similarly, the Imaging Mission Database generates depth of search maps[40] using EXOSIMS for blind-search targets such as the EXOCAT database.[41]

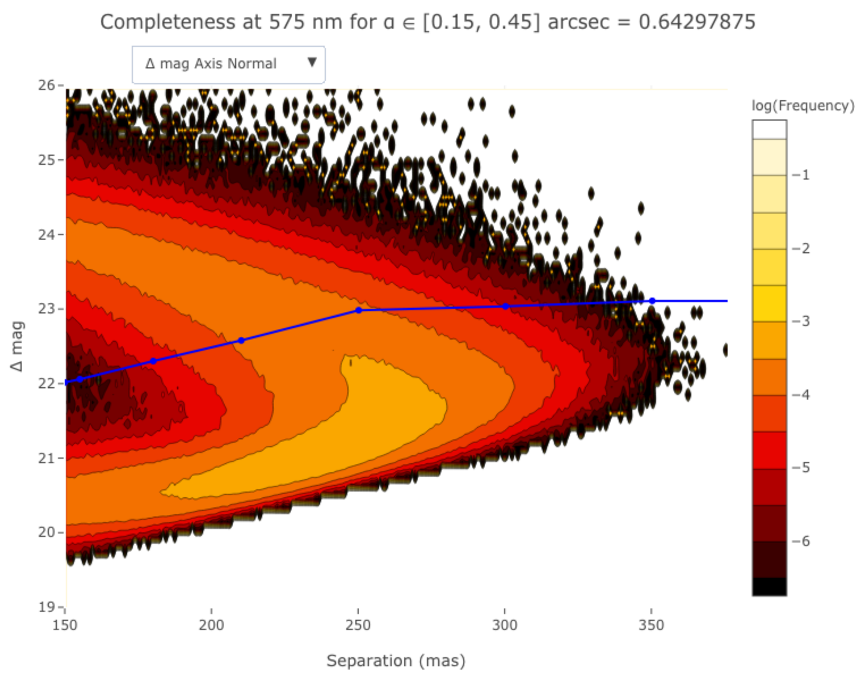

Figure 4. Map of the joint distribution of planet projected separation and Δmag for 47 Uma c generated using the Imaging Mission Database.

4. SCIENCE TARGETS

4.1 Light from Young Giant Exoplanets

Some of the substellar companions and young giant planets discovered by ground-based direct imaging surveys will be viable targets for Roman-CGI spectroscopy and photometry. This will present the first opportunity to make observations of such objects at wavelengths shorter than 0.95 μm. At the time of writing, we have identified HD 984 B, β-Pic b, HD 206893b, HR 8799e, and 51 Eri b as possible targets for Roman-CGI bandpasses 1, 2, and

3 which include spectroscopy and photometry. HR 2562b, HR 8799d, HR 8799c, κ-And b, HD 95086b, HR 3549b, HD 1160b, and HIP 65426b are possible targets for photometry in bandpass 4. We used *coolTLUSTY* to generate self-consistent 1D radiative-convective equilibrium atmosphere models for each possible target, assuming values for effective temperature, radius, and surface gravity taken from the literature and that atmospheres are clear with solar abundances. For some targets, we also compare to models with higher metallicities and with forsterite clouds. These are discussed in detail in Lacy & Burrows 2020[28] and are available publicly.For all these objects, the dominant spectral features are the pressure broadened Na and K resonant doublets around 0.59 μm and 0.77 μm respectively, especially for the cooler objects where there is stronger pressure broadening at the photosphere. For the hotter objects (above $\sim$1300 K), metal hydrides like CaH and MgH have not yet condensed and rained out, so their absorption features are present in the spectra. For intermediate temperature objects and higher metallicity hot objects, absorption features from TiO and VO also appear in the spectra. When forsterite clouds are included they increase the continuum flux ratio in the optical range and weaken gaseous absorption features. Combining optical spectroscopy and photometry with NIR and MIR observations of these objects from other instruments will aid efforts to characterize these young planets since changes to cloud properties and metallicity have different effects in the optical than at longer wavelengths.

Ideally, Roman-CGI spectroscopy will measure the strength of the $\sim$0.73 μm methane absorption feature for a reflected-light target, and constrain parameterized models incorporating cloud properties, a temperature-pressure profile, and mixing ratios of major gas-phase absorbers.[42–44] Whether this task is achieved will depend on the nature of the planets observed, the quality of data Roman-CGI collects, and the quality of auxiliary measurements like mass and orbital separation that are available from other sources. In the event that Roman-CGI performance is insufficient to constrain detailed models, Lacy et al.[27] put forward a set of models suitable for addressing a simpler task: assessing how cool giant exoplanets compare to the cool gas giants and ice giants in our own solar system. Saturn and Jupiter have higher cloud layers and lower metallicities than Uranus and Neptune. Lower metallicities decrease the amount of methane, and higher clouds make for a smaller amount of gas above the cloud layer. Together these effects weaken Jupiter and Saturn's methane absorption features compared to Neptune and Uranus. At shorter wavelengths, from 0.4-0.6 microns, Saturn and Jupiter exhibit absorption from an unidentified chromophore which reddens their appearance. This is similar to the mix of hydrocarbons, commonly termed Tholins, that give Titan its yellow-orange appearance. Retrievals on simulated observations showed that Roman-CGI observations should be able to fit a model consisting of a two-part linear combination of Jupiter and Neptune's reflective properties. One parameter sets the short wavelength weighting towards Jupiter versus Neptune and essentially depends on whether a chromophore is present or not. A second parameter sets the longer wavelength weighting towards Jupiter versus Neptune and mainly reflects the amount of methane present above the cloud layer. This approach supposes that Jupiter and Neptune represent two bounds of cool giant planet atmosphere behavior and that those observed will fall somewhere in between. Of course, this framework is over-simplified, but, in the absence of high resolution high SNR spectra, it could provide a useful starting point. A small grid of geometric albedo models in this form is also available[†], along with a GUI for calculating the light curve through out a planet's orbit and a set of models representing Jupiter's geometric albedo with constant cloud properties but varying metallicity.

4.2 Reflected Light from Cold Gas Giants

Giant Exoplanet Albedo Spectra and colors as a function of planet phase, separation, and metallicity from Cahoy et al[29] have been released along with a reference solar spectrum.

4.3 Debris Disks

The unprecedented point source sensitivity of CGI is expected to also lead to many new scattered light detections of debris disks and exozodiacal dust. Simulations of dusty systems, particularly 1 Vir, Eps Eri, HD 10647, HD 69830, HD 95086, HR 8799, and Tau Cet were prepared by a the Preparatory Science Project: The Circumstellar Environments of Exoplanet Host Stars by Chen et al[26,45] and have been publicly released and include injected giant planets. General libraries of disks[25] with varied morphology and geometry have convolved with coronagraph transmission functions have also been released publicly.

[†]https://www.astro.princeton.edu/~burrows/wfirst/index.html

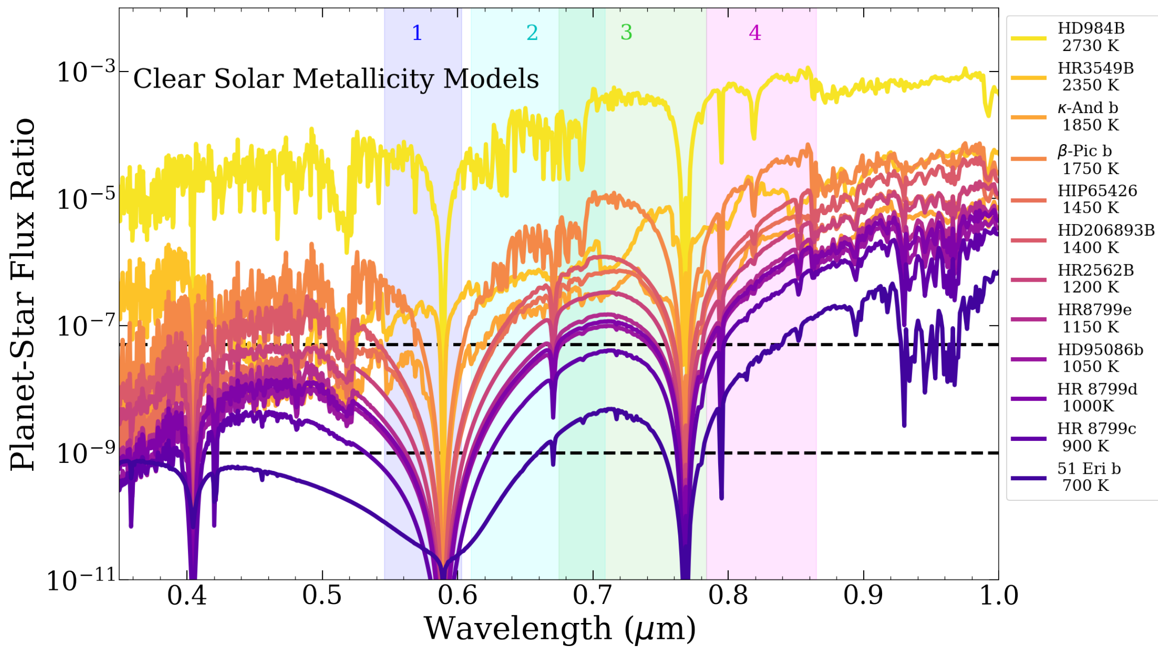

Figure 5. Model spectra for potential self-luminous targets including imaging and spectra. All models assume solar metallicity and an atmosphere free of clouds. Other model parameters are listed in table 2 of Lacy & Burrows 2020.[28] Lines for different model spectra are colored in the order of the assumed effective temperature for each object. The shaded regions indicate the Roman-CGI bandpasses. The horizontal dashed lines mark the required contrast for technology demonstration success and the engineer's best estimate of the contrast that Roman-CGI can achieve. Note that the spectral resolution of model spectra shown here are higher than the Roman-CGI spectral resolution.

4.4 Fast Extended Source Simulation with a PSF Library

The effect of the spatially varying coronagraph transmission functions on complex scenes, such as exozodiacal dust models can be simulated using public PSFs libraries.[46] These simulations are efficiently performed by generating an over-sampled scene model and applying a coronagraphic transfer function via matrix multiplication. Because of the field-dependent evolution of the PSF, a PSF must be generated for every angular offset of the pixel coordinates of the scene model. These PSFs are generated via interpolation of the PSFs available from IPAC and stored as matrices in memory. For example, an exozodiacal model can be flattened into a vector rather than a 2D array and multiplied by the matrix of interpolated PSFs since the coronagraph is still assumed to be a linear system. For details and examples of disk generation, see Milani et al.[47]

4.5 PSF subtraction

Post-processing via Karhunen-Lo‘eve Image Processing (KLIP) subtraction of residual speckles has been extensively explored for Roman[48,49] and exoplanet extraction has been one of the data challenge topics.[50] pyKLIP[51] supports generic data and the documentation currently includes an example of KLIP run on an observing scenario.

5. CONCLUSIONS

Roman CGI has has stimulated and nurtured a wide array of coronagraph and mission simulation tools. In addition to the simulation software describe above, Data Challenges[50,52,53] have allowed the community to engage and develop additional tools[‡]. Integral field spectrograph modes were considered for Roman and simulated in Coronagraph and Rapid Imaging Spectrograph in Python (`crispy`)[54] which may also prove useful for other

[‡]https://roman.ipac.caltech.edu/sims/Exoplanet_Data_Challenges.html

missions[§]. The majority of the tools described above have been developed in Python; however, other tools have been developed for estimating coronagraph noise[55] in languages such as IDL[¶]. It is hoped that the open-source availability of all these tools will allow the community to more rapidly develop science questions with Roman CGI and provide springboards for future coronagraphic missions.

ACKNOWLEDGMENTS

This research has made use of the Imaging Mission Database, which is operated by the Space Imaging and Optical Systems Lab at Cornell University. The database includes content from the NASA Exoplanet Archive, which is operated by the California Institute of Technology, under contract with the National Aeronautics and Space Administration under the Exoplanet Exploration Program, and from the SIMBAD database, operated at CDS, Strasbourg, France.[56]

Portions of this work were supported by the Roman/WFIRST Science Investigation team prime award #NNG16PJ24C. Portions of this work were supported by the Arizona Board of Regents Technology Research Initiative Fund (TRIF).

REFERENCES

[1] Spergel, D., Gehrels, N., Baltay, C., Bennett, D., Breckinridge, J., Donahue, M., Dressler, A., Gaudi, B. S., Greene, T., Guyon, O., Hirata, C., Kalirai, J., Kasdin, N. J., Macintosh, B., Moos, W., Perlmutter, S., Postman, M., Rauscher, B., Rhodes, J., Wang, Y., Weinberg, D., Benford, D., Hudson, M., Jeong, W.-S., Mellier, Y., Traub, W., Yamada, T., Capak, P., Colbert, J., Masters, D., Penny, M., Savransky, D., Stern, D., Zimmerman, N., Barry, R., Bartusek, L., Carpenter, K., Cheng, E., Content, D., Dekens, F., Demers, R., Grady, K., Jackson, C., Kuan, G., Kruk, J., Melton, M., Nemati, B., Parvin, B., Poberezhskiy, I., Peddie, C., Ruffa, J., Wallace, J. K., Whipple, A., Wollack, E., and Zhao, F., "Wide-Field InfrarRed Survey Telescope-Astrophysics Focused Telescope Assets WFIRST-AFTA 2015 Report," *ArXiv e-prints* **1503**, 3757 (Mar. 2015).

[2] Noecker, M. C., Zhao, F., Demers, R., Trauger, J., Guyon, O., and Kasdin, N. J., "Coronagraph instrument for WFIRST-AFTA," *JATIS, JATIAG* **2**, 011001 (Mar. 2016).

[3] Kasdin, N. J., Turnbull, M., Macintosh, B., Lewis, N., Roberge, A., Trauger, J., Mennesson, B., Bailey, V., Rhodes, J., Moustakas, L., Frerking, M. A., Zhao, F., Demers, R. T., and Poberezhskiy, I. Y., "The WFIRST coronagraph instrument: technology demonstration and science potential (Conference Presentation)," in [*Space Telescopes and Instrumentation 2018: Optical, Infrared, and Millimeter Wave*], **10698**, 106982H, International Society for Optics and Photonics (July 2018).

[4] Douglas, E. S., Carlton, A. K., Cahoy, K. L., Kasdin, N. J., Turnbull, M., and Macintosh, B., "WFIRST coronagraph technology requirements: status update and systems engineering approach," in [*Modeling, Systems Engineering, and Project Management for Astronomy VIII*], **10705**, 1070526, International Society for Optics and Photonics (July 2018).

[5] Bailey, V. P., Savransky, D., Debes, J., Mennesson, B., and Zellem, R., "WFIRST design reference mission: the coronagraph instrument (Conference Presentation)," in [*Techniques and Instrumentation for Detection of Exoplanets IX*], **11117**, 111170E, International Society for Optics and Photonics (Sept. 2019).

[6] Shi, F., Balasubramanian, K., Bartos, R., Hein, R., Lam, R., Mandic, M., Moore, D., Moore, J., Patterson, K., Poberezhskiy, I., Shields, J., Sidick, E., Tang, H., Truong, T., Wallace, J. K., Wang, X., and Wilson, D. W., "Low order wavefront sensing and control for WFIRST coronagraph," in [*Proc. SPIE*], 990418 (July 2016).

[7] Sidick, E., Krist, J., and Poberezhskiy, I., "WFIRST coronagraph: digging dark-holes with partially corrected pupil phase," in [*Space Telescopes and Instrumentation 2018: Optical, Infrared, and Millimeter Wave*], **10698**, 106986W, International Society for Optics and Photonics (July 2018).

[8] Bailey, V., "WFIRST CGI performance in context," (2019).

[§] https://github.com/mjrfringes/crispy

[¶] https://github.com/tdrobinson/coronagraph_noise

[9] Trauger, J., Moody, D., Krist, J., and Gordon, B., "Hybrid Lyot coronagraph for WFIRST-AFTA: coronagraph design and performance metrics," *J. Astron. Telesc. Instrum. Syst* **2**(1), 011013–011013 (2016).

[10] Balasubramanian, K., White, V., Yee, K., Echternach, P., Muller, R., Dickie, M., Cady, E., Prada, C. M., Ryan, D., Poberezhskiy, I., Kern, B., Zhou, H., Krist, J., Nemati, B., Eldorado Riggs, A. J., Zimmerman, N. T., and Kasdin, N. J., "WFIRST-AFTA coronagraph shaped pupil masks: design, fabrication, and characterization," *J. Astron. Telesc. Instrum. Syst* **2**(1), 011005–011005 (2015).

[11] Poberezhskiy, I. and et al., "CGI engineering design and operational concept," in [*Proc SPIE*], **11443**, 11443–195 (2020).

[12] Kasdin, N. J. and et al., "The WFIRST coronagraph instrument (CGI) technology demonstration," in [*Proc SPIE*], **11443**, 11443–194 (2020).

[13] Krist, J. E., Nemati, B., and Mennesson, B. P., "Numerical modeling of the proposed WFIRST-AFTA coronagraphs and their predicted performances," *JATIS* **2**, 011003 (Oct. 2015).

[14] Krist, J. E., "PROPER: an optical propagation library for IDL," in [*Proc. SPIE*], **6675**, 66750P–66750P–9 (2007).

[15] Krist, J., Riggs, A. J., McGuire, J., Tang, H., Amiri, N., Gutt, G., Marchen, L., Marx, D., Nemati, B., Saini, N., Sidick, E., and Zhou, H., "WFIRST coronagraph optical modeling," in [*Techniques and Instrumentation for Detection of Exoplanets VIII*], **10400**, 1040004, International Society for Optics and Photonics (Sept. 2017).

[16] Riggs, A. J. E., Ruane, G. J., Sidick, E., Coker, C. T., and Kern, B. D., "Fast Linearized Coronagraph Optimizer (FALCO) I. a software toolbox for rapid coronagraphic design and wavefront correction," in [*Proc. SPIE*], **10698**, 106982V (2018).

[17] Pogorelyuk, L., Pueyo, L., and Kasdin, N. J., "On the effects of pointing jitter, actuator drift, telescope rolls, and broadband detectors in dark hole maintenance and electric field order reduction," *JATIS* **6**, 039001 (July 2020). Publisher: International Society for Optics and Photonics.

[18] Perrin, M. D., Soummer, R., Elliott, E. M., Lallo, M. D., and Sivaramakrishnan, A., "Simulating point spread functions for the james webb space telescope with webbpsf," in [*Space Telescopes and Instrumentation 2012: Optical, Infrared, and Millimeter Wave*], **8442**, 84423D, International Society for Optics and Photonics (2012).

[19] Perrin, M. D., Sivaramakrishnan, A., Lajoie, C.-P., Elliott, E., Pueyo, L., Ravindranath, S., and Albert, L., "Updated point spread function simulations for jwst with webbpsf," in [*Space Telescopes and Instrumentation 2014: Optical, Infrared, and Millimeter Wave*], **9143**, 91433X, International Society for Optics and Photonics (2014).

[20] Sirbu, D., Thomas, S., Belikov, R., and Bendek, E., "Techniques for High Contrast Imaging in Multi-Star Systems II: Multi-Star Wavefront Control," *ApJ* **849**(2) (2017).

[21] Sirbu, D., Belikov, R., Bendek, E., Henze, C., Riggs, A. J. E., and Shaklan, S., "Multi-Star Wavefront Control for the Wide-Field Infrared Survey Telescope," in [*Proc. SPIE*], **10698**, 106982F (2018).

[22] Savransky, D., Delacroix, C., and Garrett, D., "EXOSIMS: Exoplanet Open-Source Imaging Mission Simulator," *Astrophysics Source Code Library* , ascl:1706.010 (June 2017).

[23] Savransky, D. and Garrett, D., "WFIRST-AFTA coronagraph science yield modeling with EXOSIMS," *Journal of Astronomical Telescopes, Instruments, and Systems* **2**, 011006 (Jan. 2016).

[24] Savransky, D., Gascón, C., Kinzly, N., Batalha, N., Lewis, N., and Marley, M., "Exploration of the dynamical phase space of stars with known planets," in [*Techniques and Instrumentation for Detection of Exoplanets IX*], Shaklan, S. B., ed., **11117**, 438 – 453, International Society for Optics and Photonics, SPIE (2019).

[25] Mennesson, B., Kasdin, N. J., Macintosh, B., Turnbull, M., Douglas, E., Stark, C., Rizzo, M., Krist, J., Trauger, J., Rhodes, J., Moustakas, L., Frerking, M. A., Zhao, F., Poberezhskiy, I. Y., Demers, R. T., Roberge, A., Debes, J. H., Nemati, B., Zimmerman, N., Cahoy, K., and Bailey, V., "The WFIRST coronagraph instrument: a major step in the exploration of sun-like planetary systems via direct imaging," in [*Space Telescopes and Instrumentation 2018: Optical, Infrared, and Millimeter Wave*], MacEwen, H. A., Lystrup, M., Fazio, G. G., Batalha, N., Tong, E. C., and Siegler, N., eds., 88, SPIE, Austin, United States (Aug. 2018).

[26] Chen, "WFIRST Preparatory Science Project: The Circumstellar Environments of Exoplanet Host Stars."

[27] Lacy, B., Shlivko, D., and Burrows, A., "Characterization of Exoplanet Atmospheres with the Optical Coronagraph on *WFIRST*," *AJ* **157**, 132 (Mar. 2019).

[28] Lacy, B. and Burrows, A., "Prospects for Directly Imaging Young Giant Planets at Optical Wavelengths," *ApJ* **892**, 151 (Apr. 2020).

[29] Cahoy, K. L., Marley, M. S., and Fortney, J. J., "Exoplanet Albedo Spectra and Colors as a Function of Planet Phase, Separation, and Metallicity," *ApJ* **724**, 189–214 (Nov. 2010).

[30] Krist, J., "PROPER: an optical propagation library for IDL," in [*Proc. SPIE*], **6675**, 66750P (2007).

[31] Krist, J., Effinger, R., Kern, B., Mandic, M., McGuire, J., Moody, D., Morrissey, P., Poberezhskiy, I., Riggs, A. J., Saini, N., Sidick, E., Tang, H., and Trauger, J., "WFIRST coronagraph flight performance modeling," in [*Space Telescopes and Instrumentation 2018: Optical, Infrared, and Millimeter Wave*], **10698**, 106982K, International Society for Optics and Photonics (July 2018).

[32] Saini, N., Anderson, K., Chang, Z., Gutt, G., and Nemati, B., "IMPipeline: an integrated STOP modeling pipeline for the WFIRST coronagraph (Conference Presentation)," in [*Techniques and Instrumentation for Detection of Exoplanets VIII*], **10400**, 1040008, International Society for Optics and Photonics (Oct. 2017).

[33] Harris, C. R., Millman, K. J., van der Walt, S. J., Gommers, R., Virtanen, P., Cournapeau, D., Wieser, E., Taylor, J., Berg, S., Smith, N. J., Kern, R., Picus, M., Hoyer, S., van Kerkwijk, M. H., Brett, M., Haldane, A., del R'ıo, J. F., Wiebe, M., Peterson, P., G'erard-Marchant, P., Sheppard, K., Reddy, T., Weckesser, W., Abbasi, H., Gohlke, C., and Oliphant, T. E., "Array programming with NumPy," *Nature* **585**, 357–362 (Sept. 2020).

[34] Thomas, S., Belikov, R., and Bendek, E., "Techniques for High Contrast Imaging in Multi-Star Systems I: Super-Nyquist Wavefront Control," *ApJ* **810**(1) (2015).

[35] Douglas, E. S. and Perrin, M. D., "Accelerated modeling of near and far-field diffraction for coronagraphic optical systems," in [*Proc SPIE*], MacEwen, H. A., Lystrup, M., Fazio, G. G., Batalha, N., Tong, E. C., and Siegler, N., eds., 100, SPIE, Austin, United States (July 2018).

[36] Perrin, M., Long, J., Douglas, E., Sivaramakrishnan, A., and Slocum, C., "POPPY: physical optics propagation in Python." ASCL (2016).

[37] Nemati, B., Krist, J. E., and Mennesson, B., "Sensitivity of the WFIRST coronagraph performance to key instrument parameters," in [*Techniques and Instrumentation for Detection of Exoplanets VIII*], **10400**, 1040007, International Society for Optics and Photonics (Sept. 2017).

[38] Nemati, B., Stahl, H. P., Stahl, M. T., Ruane, G. J. J., and Sheldon, L. J., "Method for deriving optical telescope performance specifications for Earth-detecting coronagraphs," *JATIS* **6**, 039002 (Aug. 2020). Publisher: International Society for Optics and Photonics.

[39] Batalha, N. E., Smith, A. J., Lewis, N. K., Marley, M. S., Fortney, J. J., and Macintosh, B., "Color classification of extrasolar giant planets: Prospects and cautions," *The Astronomical Journal* **156**(4), 158 (2018).

[40] Garrett, D., Savransky, D., and Macintosh, B., "A simple depth-of-search metric for exoplanet imaging surveys," *The Astronomical Journal* **154**(2), 47 (2017).

[41] Turnbull, M. C., "Exocat-1: The nearby stellar systems catalog for exoplanet imaging missions," *arXiv preprint arXiv:1510.01731* (2015).

[42] Lupu, R. E., Marley, M. S., Lewis, N., Line, M., Traub, W. A., and Zahnle, K., "Developing Atmospheric Retrieval Methods for Direct Imaging Spectroscopy of Gas Giants in Reflected Light. I. Methane Abundances and Basic Cloud Properties," *The Astronomical Journal* **152**, 217 (Dec. 2016).

[43] Nayak, M., Lupu, R., Marley, M. S., Fortney, J. J., Robinson, T., and Lewis, N., "Atmospheric Retrieval for Direct Imaging Spectroscopy of Gas Giants in Reflected Light. II. Orbital Phase and Planetary Radius," *PASP* **129**, 034401 (Jan. 2017). Publisher: IOP Publishing.

[44] Damiano, M. and Hu, R., "ExoRel$^{\Re}$: A Bayesian Inverse Retrieval Framework for Exoplanetary Reflected Light Spectra," AJ **159**, 175 (Apr. 2020).

[45] Chen, C., "The Circumstellar Environments of Exoplanet Host Stars," *NASA WPS Proposal* , 14–WPS14–43 (2014).

[46] Douglas, E. S., Debes, J., Milani, K., Xin, Y., Cahoy, K. L., Lewis, N. K., and Macintosh, B., "Simulating the effects of exozodiacal dust in WFIRST CGI observations," in [*Techniques and Instrumentation for Detection of Exoplanets IX*], **11117**, 111170K, International Society for Optics and Photonics (Sept. 2019).

[47] Milani, K. and Douglas, E. S., "Faster imaging simulation through complex systems: a coronagraphic example," in [*Optical Modeling and Performance Predictions XI*], **11484**, 1148405, International Society for Optics and Photonics (Aug. 2020).

[48] Ygouf, M., Pueyo, L., Soummer, R., Perrin, M. D., Marel, R. v. d., and Macintosh, B., "Data processing and algorithm development for the WFIRST-AFTA coronagraph: reduction of noise free simulated images, analysis and spectrum extraction with reference star differential imaging," in [*Techniques and Instrumentation for Detection of Exoplanets VII*], **9605**, 96050S, International Society for Optics and Photonics (Sept. 2015).

[49] Ygouf, M., Zimmerman, N. T., Pueyo, L., Soummer, R., Perrin, M. D., Mennesson, B. E., Krist, J. E., Vasisht, G., Nemati, B., and Macintosh, B. A., "Data processing and algorithm development for the WFIRST coronagraph: comparison of RDI and ADI strategies and impact of spatial sampling on post-processing," in [*Space Telescopes and Instrumentation 2016: Optical, Infrared, and Millimeter Wave*], **9904**, 99045M, International Society for Optics and Photonics (July 2016).

[50] Mandell, A. M., Turnbull, M., Zimmerman, N. T., Hildebrandt, S., Rizzo, M., Roberge, A., and Merrelli, A., "The WFIRST Coronograph Exoplanet Data Challenge," **233**, 140.44 (Jan. 2019). Conference Name: American Astronomical Society Meeting Abstracts #233.

[51] Wang, J. J., Ruffio, J.-B., De Rosa, R. J., Aguilar, J., Wolff, S. G., and Pueyo, L., "pyKLIP: PSF Subtraction for Exoplanets and Disks," *Astrophysics Source Code Library* , ascl:1506.001 (June 2015).

[52] Hildebrandt, S., Turnbull, M., and Team, E. D. C., "WFIRST: Exoplanet Data Challenge. Atmospheric retrieval results," in [*American Astronomical Society Meeting Abstracts #231*], **231** (Jan. 2018).

[53] Girard, J. and et al., "The 2019 WFIRST exoplanet imaging data challenge: What have we learned?," in [*Proc SPIE*], **11443**, 11443–146 (2020).

[54] Rizzo, M. J., Groff, T. D., Zimmermann, N. T., Gong, Q., Mandell, A. M., Saxena, P., McElwain, M. W., Roberge, A., Krist, J., Riggs, A. J. E., Cady, E. J., Prada, C. M., Brandt, T., Douglas, E., and Cahoy, K., "Simulating the WFIRST coronagraph integral field spectrograph," **10400**, 104000B, International Society for Optics and Photonics (Sept. 2017).

[55] Robinson, T. D., Stapelfeldt, K. R., and Marley, M. S., "Characterizing Rocky and Gaseous Exoplanets with 2-meter Class Space-based Coronagraphs: General Considerations," *arXiv:1507.00777 [astro-ph]* (July 2015). arXiv: 1507.00777.

[56] Wenger, M., Ochsenbein, F., Egret, D., Dubois, P., Bonnarel, F., Borde, S., Genova, F., Jasniewicz, G., Laloë, S., Lesteven, S., et al., "The simbad astronomical database-the cds reference database for astronomical objects," *Astronomy and Astrophysics Supplement Series* **143**(1), 9–22 (2000).